Power-based Model for Temperature Prediction in FSW

Power-based Model for Temperature Prediction in FSW

D Ambrosio[1], V Wagner[1], G Dessein[1] , A Tongne[1], M Fazzini[1], C Garnier[1], O Cahuc[2]

[1] Laboratoire Génie de Production, INP/ENI Tarbes, 65016 Tarbes, France
[2] University of Bordeaux, Institute of mechanics and engineering (I2M), CNRS, 33400 Talence, France
Email: dambrosi@enit.fr

Abstract. This paper describes a thermal numerical model accessible to all users for predicting temperature in friction stir welding from the power, material thermal properties, process parameters, tool, and plate dimensions. Starting with the information obtained from the machine, power or torque, the heat flux is modeled as a circular moving source with a diameter equal to that of the shoulder. The model calibrated in a specific setup (CNC machine) successfully predicted without recalibration the weld temperature field in another one (robot). The simple thermal model was applied without recalibration to data available in the literature to test its effectiveness. The results obtained with this model are promising, although more tests are needed to cover all possible varieties of tool geometries and material thickness. If extended over a broader range of configurations (i.e., process parameters and tool-workpiece geometries), it could be a handy tool for all FSW users. The tool may help study the thermal cycles in the heat affected zone that influence final mechanical properties and make it easier to identify optimal parameters if the desired optimal peak temperatures are determined.

1. Introduction

The friction stir welding (FSW) process continues to grow, and more and more industries are becoming interested in it. Thanks to the maturity achieved after more than thirty years of development, today, the process seems much more accessible to all users. However, the difficulties related to the process remain many. Depending on the welding material and its thickness, the tool and the machine, the optimal parameters changes [1]. The friction stir welding outcomes are strongly related to the temperature reached in the nugget zone [2]. If proper temperature ranges are achieved, proper material flow during agitation can be ensured, and if not, a defective joint is likely to be obtained [3]. Similarly, in heat-treatable aluminium alloys, the mechanical properties of friction stir welds are strongly related to the heat affected zones, the weaker zone in joint [4]. The severity and the duration of the thermal cycle undergone by the welding material is responsible for microstructural modifications leading to certain mechanical properties [5]. For all these reasons, the thermal modeling and simulation of the process continue to be an essential tool to predict temperature reached in the various zone that composes the weld. Over time, various more or less complex thermal models have been proposed to predict the temperature generated by a given experimental setup. Some of these have considered contact conditions, only friction [6,7], or both friction and plastic deformation, by introducing the concepts of sticking and slipping [8,9] and rely on temperature-dependent physical quantities generated during the process (yield strength, axial force, etc.). In other cases, punctual heat sources were used in which the heat source was the power and it was tuned to minimize differences between model end experiments [10] or directly the power obtained by the machine, calibrating the

model through boundary conditions [11]. In all these cases, the respective models were calibrated on experiments done under specific conditions, and no comparisons to other cases already available in the literature were proposed. Also, many of them are based on complex models and not easily maneuverable by people not trained in modeling. For this reason, in this work, a straightforward thermal model is proposed for the prediction of the temperature in an FSW bead, given the power required for the execution of the joint and the setup characteristics (i.e., welding parameters, tool geometry, workpiece geometry and properties, backing plate). The model is calibrated with a specific experimental setup, validated with additional experiments on the same setup, extended and validated to a different setup, and finally compared to the literature.

2. Model description

2.1. Moving heat source

A finite element framework in ABAQUS™ has been used to model and simulate the thermal fields in FSW. The heat source is the mechanical power (P) obtained from the machine. An efficiency parameter η is used to calibrate the model and express what percentage of this mechanical work is converted into heat (P_{heat}). In order to calculate the surface heat flux (φ), P_{heat} is divided by the tool surface, *considering only the shoulder and the pin lateral surface, which generally represents 90% of the total surface and responsible for the heat generation.* For the sake of simplicity, features such as grooves and threads are not considered. The surface heat flux is applied to the top of the welded plates on a surface equal to the shoulder without considering the pin and moves at a speed equal to the welding speed. In these assumptions, in commercial software to perform thermal analysis, it is sufficient to model the welding plates, assign them thermal properties according to the considered material and create a moving surface heat flux. Regarding the tool contact that is not modeled here, thermal losses through the tool are taken into account through the efficiency parameter. The thermal field obtained at the top of the plates and the FSW joint cross-section running the simulation is shown in Figure 1.

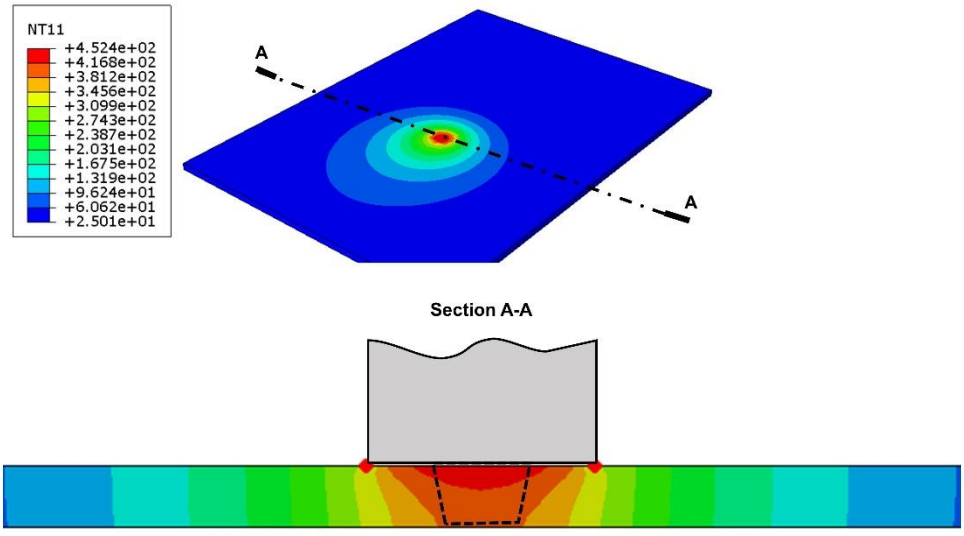

Figure 1. Plot obtained from the simulation. The thermal field in the upper plates and in the cross-section. Temperature in °C.

2.2. Boundary conditions

The boundary conditions are represented by the losses that occur with the air (lateral and upper surface of the plates) and the support system (lower surface here divided into two parts, the central one in contact with steel and the lateral part aluminum). For simplicity, these losses are all incorporated into a contact condition through a convection coefficient. These coefficients have been taken from previous

work [11], 15 and 1000 W m^{-2} $°C^{-1}$ for air and steel, respectively. The aluminum one was set to 100 W m^{-2} $°C^{-1}$ to improve the prediction in the heating and cooling cycle of the model, but it does not significantly influence the peak temperature. The interaction with the clamping system was neglected while the initial temperature in the plates was set at 25 °C.

3. Experimental

3.1. CNC lathe machine

The tests were performed on an adapted CNC lathe machine, Somab Genymab 900, in position control (Figure 2). The employed process parameters and the measured mechanical power are listed in Table 1. The experimental campaign consisted of ten bead-on-plate tests performed on 3 mm sheets (200 mm long and 180 mm large), five on AA7075-T6, and five on AA6082-T6. Of these ten tests, two from each material were used to calibrate η (C1 to C4). The validation was made on the remaining six tests (C5 to C10).

Table 1. Process parameters employed in the various experiments. Base material (BM), rotational speed (N), welding speed (v), plunge depth, axial force (F_z) and mechanical power (P)

Config	**BM** (AA)	**N** (rpm)	**v** (mm/min)	**d** (mm) / **F_z** (kN)	**P** (W)
C1	7075	500	180	0.3 mm	945
C2	7075	1500	180	0.2 mm	1060
C3	6082	1500	180	0.2 mm	1240
C4	6082	2000	180	0.1 mm	1200
C5	7075	1000	180	0.2 mm	1002
C6	7075	500	120	0.2 mm	824
C7	7075	1000	240	0.2 mm	999
C8	6082	1000	180	0.3 mm	1253
C9	6082	1000	240	0.1 mm	1140
C10	6082	1500	360	0.1 mm	1255
K1	7075	800	60	6 kN	951
K2	7075	1400	60	5.5 kN	1112
K3	7075	1400	180	7.5 kN	1281

Figure 2. CNC lathe machine setup

Figure 3. KUKA robot setup

3.2. KUKA robot

The runs were carried out on a Kuka KR500-3MT robot with an Actemium BPA-6700 spindle in force control (Figure 3). The employed process parameters and the measured mechanical power are listed in Table 1. The experimental campaign consisted of three bead-on-plate tests performed on 3 mm AA7075-T6 sheets (200 mm long and 180 mm large). Temperature measurements were used to validate the model without recalibrating the parameter for the new configuration.

3.3. Tool and thermocouple

The H13 steel tool was characterized by an 11,5 mm grooved shoulder diameter and a 2.8 mm height frustum shape threaded pin with an upper and lower diameter of 5 and 4 mm. In both experimental configurations, the support system was made of mild steel in the central part surrounded by aluminum. The width of the steel backing plate was different in the two setups, 40 and 60 mm, and this difference was considered when applying the boundary conditions.

In tests performed with the CNC machine, the thermocouples were embedded in the sheets, grooves 2 mm deep, and at a distance of 1 mm from the welding line on the advancing (AS) and retreating side (RS). Post-welding, the thermocouples' final position was determined through computer tomography. They were found about 2.5 mm away from the center due to the pin push action before its arrival. In contrast, the thermocouples were placed between sheets and backing plate in the robot tests, thus measuring the temperature on the bottom surface. The thermocouples distance from the welding line was 3 and 6 mm on the AS and 7 mm on the RS. Transient temperatures were recorded using K-type thermocouples (accuracy ±2 °C). The measurements were acquired by a National Instruments DAQ system at 15 Hz.

4. Results and discussion

4.1. CNC lathe machine

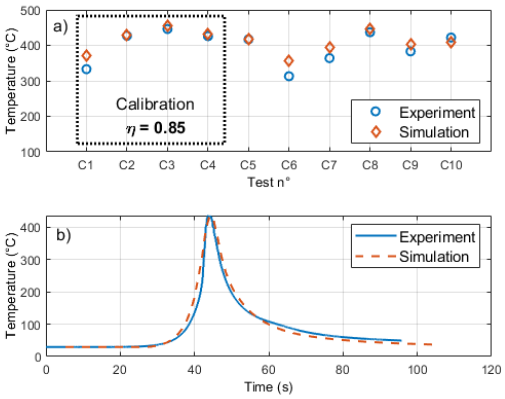

Figure 4. a) comparison between experimental and simulated peak temperatures in test performed on the CNC lathe machine, b) C2 configuration showing the experimental and simulated thermal cycles.

The first four C1-C4 tests were chosen for model calibration. Given the very similar values obtained at both sides, the peak temperature reported in Figure 4a was calculated as the average peak temperature between the two thermocouples. An optimal value of η equal to 0.85 has been chosen in the calibration to minimize the differences between simulated and measured peak temperatures. The same value has been used for all the other cases for validation. In Figure 3a, it can be observed the good approximation offered by the model independently from the material, rotational speed, and welding speed. In eight out of ten tests, the error is less than 5%, confirming a reasonable estimate of the maximum temperature at 2.5 mm from the welding line. Moreover, the two cases in which the prediction error approaches 10% (C1 and C6) are characterized by rotational speeds of 500 rpm (the lowest tested) and the same AA7075-T6 material, thus showing a problem at low rotational speeds. In any case, it is plausible to think that the efficiency parameter is inevitably dependent on both the process parameters and the tool-workpiece materials. However, without considering this dependence, the results are satisfying considering its application to two alloys and ten welding configurations. In

Figure 4b, the comparison of the experimental and simulated thermal cycles of the C2 configuration is displayed. The thermal cycle is predicted to a good approximation.

4.2. KUKA robot

To verify the model's effectiveness, three tests were performed with the same tool and 3 mm-thick AA7075-T6 slabs but in a different configuration (i.e., different machine used to perform the welding, support system, and clamping system). The comparison of measured and simulated peak temperatures is remarkably successful (Figure 5a), with an error on average equal to 5%. The differences due to the system and the different positions of the thermocouples did not reduce the model's prediction ability without any kind of recalibration (i.e., η=0.85). Similarly, the thermal cycle for all three thermocouples is predicted to a good approximation, as shown in Figure 5b.

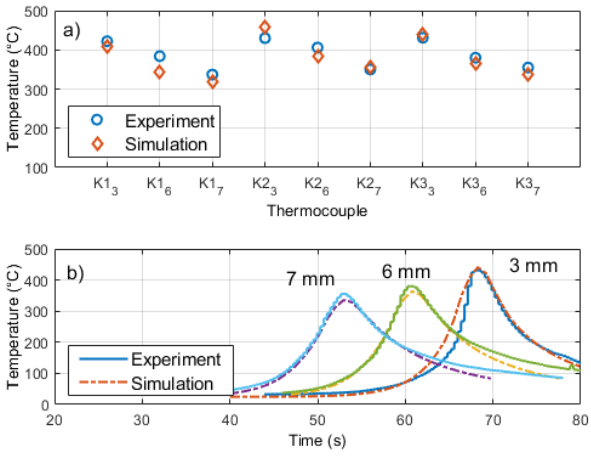

Figure 5. a) comparison between experimental and simulated peak temperatures in test performed on the KUKA robot ($Ki_{x,}$ i is the test number while x is the thermocouple position), b) K3 configuration showing the experimental and simulated thermal cycles.

4.3. Comparison with literature

Among the few works wherein both temperature measurements and any power or torque measurements are shared, [12] was chosen. Although the most information contained is related to the peak temperatures measured in the nugget zone, through thermocouples embedded in the tool, while the model has been calibrated and validated with temperatures outside the nugget zone, it was decided to evaluate the model without any recalibration. In addition, the process parameter combinations vary widely, not to mention that the plates' thickness has doubled (from 3 mm to more than 6 mm) as well as the tool geometry has also changed. Despite all of these differences, in six out of ten combinations, the prediction error of the peak temperature in the nugget zone is on average 5% (Figure 6a).

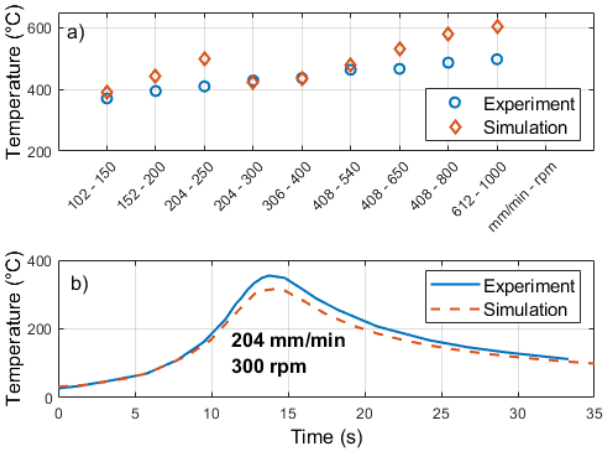

Figure 6. a) comparison between experimental and simulated peak temperatures in [12], b) comparison between experimental and simulated thermal cycles.

However, in other cases, the temperature is too high as the model has no upper limit for heat generation. In the physics of the process, once temperatures above solidus are reached in the nugget zone (around 480 °C for the alloy tested in [12], AA7050), heat generation drops dramatically, and then the temperature stabilizes. In contrast, the model's predictive ability on the heating and cooling cycles is established by comparing the thermal cycle, displayed in Figure 6b, with a measurement taken 6 mm from the welding line.

5. Conclusion

The excellent prediction capability of thermal cycles generated during FSW through a simple thermal FEM model based on a single input has been demonstrated. Its robustness has been verified in various contexts predicting both heat-affected zone and nugget zone temperatures. However, there is a need to incorporate an upper bound into the heat generation to improve the prediction of nugget zone temperature to avoid too high and too far temperatures above the solidus one. Furthermore, this model could be enhanced by studying the efficiency parameter dependence on the process parameters and the tool-workpiece coupling (both material and dimensions). The strength of this macroscopic approach is that it is purely thermal and disregards physical quantities that vary with temperature or are challenging to determine (i.e., yield strength, viscosity, etc.) or the interface tool-workpiece condition without losing prediction quality. In addition, if reliable empirical or analytical models defining the dependence of power on process parameters in a specific configuration are developed, the temperatures achieved with certain process parameters could be easily traced with this thermal model. Hence, in future works, the thermal model can be improved to estimate the mechanical properties of friction stir welding as a function of the thermal cycle induced by the chosen configuration. Also, if optimal temperature ranges to be guaranteed in the nugget zone can be defined, the model could identify suitable process parameters.

6. References

[1] Leitão C, Louro R, Rodrigues D M 2012 *Mater. Des.* **37** 402–409.
[2] Fehrenbacher A., Duffie N A, Ferrier N J, Pfefferkorn F E, Zinn M R 2014 *Int. J. Adv. Manuf. Technol.* **71(1–4)** 165–179.
[3] Ambrosio D, Wagner V, Garnier C, Jacquin D, Tongne A., Fazzini M., Cahuc O, Dessein G 2020 *WELD. WORLD.* **64(5)** 773–784.
[4] Simar A, Bréchet Y, de Meester B, Denquin A, Pardoen T (2008) *Mater. Sci. Eng. A* **486(1–2)**, 85–95
[5] Ambrosio D, Garnier C, Wagner V, Aldanondo E, Dessein G, Cahuc O 2020 *Int. J. Adv. Manuf. Technol.* **111(5–6)** 1333–1350
[6] Song M, Kovacevic R 2003 *Int. J. Mach. Tools Manuf.* **43(6)** 605–615
[7] Zhang X X, Xiao B L, Ma Z Y 2011 *Metall. Mater. Trans. A Phys. Metall. Mater. Sci.* **42(10)** 3218–3228
[8] Schmidt H, Hattel J 2005 *Sci. Technol. Weld. Join.* **10(2)** 176–186
[9] Zhang P, Yan H, Li C, Yu Z, Lu Q 2017 *Sci. Eng. Compos. Mater.* **24(3)** 439–446
[10] Vilaça P, Quintino L, Dos Santos J F 2005 *J. Mater. Process. Technol.* **169(3)** 452–465
[11] Khandkar M Z H, Khan J A, Reynolds A P 2003 *Sci. Technol. Weld. Join.* **8(3)** 165-174
[12] Upadhyay P, Reynolds A P 2010 *Mater. Sci. Eng. A* **527(6)** 1537–1543.

Acknowledgments

This project received funding from the European Union's Marie Skłodowska-Curie Actions (MSCA) Innovative Training Networks (ITN) H2020-MSCA-ITN-2017 under the grant agreement N°764979.